TRENDS IN SCIENCES 2026; 23(8): 12838
https://doi.org/10.48048/tis.2026.12838 RESEARCH ARTICLE

Toothpaste Containing Green-synthesized Silver Nanoparticle using *Moringa oleifera* Leaf Extract and Ulvan: Formulation, Characterization, Antifungal Activity and Stability Test

Nuur Aanisah, Salsabila Jaya, Evelyn Aprilly Tanan and Evi Sulastri*

Department of Pharmacy, Faculty of Mathematics and Natural Sciences, Tadulako University, Palu 94118, Indonesia

(*Corresponding author's e-mail: evisulas3@gmail.com)

Received: 28 November 2025, Revised: 25 December 2025, Accepted: 1 January 2026, Published: 20 March 2026

Abstract

This study addresses the need to enhance the antifungal activity of toothpaste formulations while ensuring the use of safe and biocompatible synthesis approaches**.** Therefore, this study aimed to develop silver nanoparticles (AgNPs) via a green approach to improve antifungal performance in toothpaste formulations, using *Moringa oleifera* leaf extract as a safe bioreductor and ulvan as a stabilizing agent. *Moringa oleifera* leaves were extracted by maceration using 96% ethanol, while ulvan was isolated from *Ulva lactuca* through acid extraction and enzymatic treatment. AgNPs were synthesized at varying extract concentrations (0.3% - 0.7%), labeled as E1 - E5, and characterized using UV-Vis spectroscopy, particle size analysis, zeta potential measurement, FTIR, and PXRD. The AgNP formation was confirmed by a color change to reddish-brown and a distinct SPR band, with λmax shifting with increasing extract concentration. Particle size ranged from 438 - 699 nm, indicating aggregation, while zeta potential values (−4.9 to −12.6 mV) suggested moderate colloidal stability. FTIR analysis of alginate beads containing AgNPs revealed characteristic O–H, COO^-, and C–O–C bands, confirming metal-carboxylate interactions, whereas PXRD showed crystalline Ag peaks. Toothpaste formulations (F1 - F5) incorporating the beads were evaluated for physical properties, antifungal activity, and stability. All formulas exhibited acceptable organoleptic characteristics, homogeneous texture, and the physical properties meeting SNI standards. Antifungal testing demonstrated inhibition zones of 19 - 22 mm, with higher AgNP concentrations yielding stronger activity. Stability testing over 14 days indicated no significant changes in color, odor, homogeneity, pH, foaming, or spreadability, with slight decreases in viscosity. In conclusion, F3 showed the most favorable balance of physical stability, AgNP incorporation (6.01 ± 0.08 mg/L), and antifungal performance. These findings demonstrate that green-synthesized AgNPs encapsulated in alginate beads have strong potential for incorporation into safe and effective antifungal toothpaste formulations.

Keywords: Alginate beads, Green synthesis, *Moringa oleifera*, Silver nanoparticle, Toothpaste, Ulvan

Introduction

Toothpaste is one of the most widely used oral care products for preventing plaque accumulation, inhibiting the growth of pathogenic microorganisms, and maintaining oral hygiene. Although various antimicrobial agents have been incorporated into conventional toothpaste formulations, increasing microbial resistance and the high prevalence of oral fungal infections, particularly those caused by *Candida albicans*, highlight the need for alternative antimicrobial agents that are both effective and safe. Silver nanoparticles (AgNPs) have been extensively reported to possess broad-spectrum antimicrobial activity against both bacterial and fungal pathogens. Their strong antimicrobial efficacy is attributed to the release of silver ions (Ag^+), which disrupt microbial cell walls and generate reactive oxygen species (ROS) that lead to pathogen cell death [1,2]. Previous studies have shown that the non-selective antimicrobial action and potential

cytotoxicity of AgNPs are strongly dependent on both exposure time and concentration [3]. In oral-care applications, the cleansing and antimicrobial effects of AgNP-containing toothpastes are essentially instantaneous, reducing microbial load within minutes during brushing and generally not exhibiting toxic effects at appropriately low concentrations [3,4] These characteristics support the suitability of AgNPs as functional antimicrobial additives in toothpaste formulations.

As demonstrated by [5], AgNPs synthesized using *Aloe vera* extract and 1 mM $AgNO_3$ exhibited antifungal activity against *Candida albicans*, producing inhibition zones ranging from 10 to 22 mm, indicating their strong potential for application in oral healthcare formulations. However, conventional synthesis of AgNPs often relies on hazardous chemicals that may pose environmental risks. To address this issue, green synthesis has emerged as a more environmentally friendly approach, utilizing plant-derived biomolecules as reducing and stabilizing agents. This method employs natural materials such as plant extracts, microbes, or polysaccharides to reduce metal salts into nanoparticles while providing intrinsic stabilization [6-8]. Among these, *Moringa oleifera* leaves represent a promising natural source for AgNP synthesis.

Moringa oleifera leaves are rich in polyphenols, flavonoids, proteins, and other phytochemicals capable of reducing Ag^+ to Ag^0 while simultaneously stabilizing the resulting nanoparticles [9]. Natural compounds extracted from plants or bacteria act as bioreductants to convert metal precursors into nanoparticles [10]. As reported by [11], *Moringa oleifera* leaf extract successfully produced stable AgNPs in solution. Meanwhile, ulvan, a sulfated polysaccharide derived from green seaweed (*Ulva lactuca*) can function as a natural stabilizer. [12] demonstrated that ulvan not only facilitates green fabrication of AgNPs but also provides superior nanoparticle stabilization compared to synthetic stabilizers such as citric acid, due to its ability to form protective layers that prevent aggregation. The combined use of *Moringa* extract and ulvan is therefore expected to produce AgNPs that are stable, uniform, and exhibit strong antimicrobial activity.

To maintain nanoparticle stability within a product formulation, AgNPs can be encapsulated into alginate beads serving as a carrier system. Alginate is a natural biopolymer capable of forming cross-linked beads that entrap nanoparticles, protecting them from degradation or aggregation while enabling controlled release during application in the oral cavity. This controlled release mechanism may enhance and prolong the antimicrobial effect [13]. AgNP-loaded alginate beads can subsequently be incorporated into toothpaste formulations, which must undergo physicochemical evaluation such as appearance, homogeneity, pH, viscosity, spreadability, and foaming ability to ensure product quality, usability, and storage stability. In addition, FTIR and XRD analyses are needed to confirm successful nanoparticle loading and to characterize chemical and structural properties of the beads.

Although numerous studies have explored green synthesis of AgNPs and their applications in healthcare, few have integrated all stages comprehensively from synthesis, encapsulation, and characterization to incorporation in toothpaste formulations. This study addresses this gap by adopting an integrated approach that examines the relationship between synthesis conditions (0.3% - 0.7% *Moringa* extract and 1% ulvan), AgNP characteristics (maximum wavelength, particle size, zeta potential, and antifungal activity against *Candida albicans*), the structural properties of AgNP-loaded alginate beads (FTIR/XRD profiles), and the performance of the final toothpaste formulation (physical quality and stability testing). Through this approach, the study aims to develop a stable, safe, and environmentally friendly antimicrobial toothpaste capable of helping prevent fungal infections in the oral cavity.

Materials and methods

Extraction of moringa leaves using the maceration method

Samples of *Moringa oleifera* leaves were obtained from Sibedi Village, Marawola District, Sigi Regency. The collected leaves were fresh, green, and free from physical damage. After collection, the leaves were manually sorted to remove unwanted parts, then washed thoroughly under running clean water to eliminate dust and surface contaminants. The cleaned leaves were subsequently air-dried indoors in a shaded environment to avoid direct sunlight exposure. The dried leaves were ground using a blender to obtain a fine powder and sieved through a 60-mesh sieve. The resulting leaf

powder was macerated in 96% ethanol at a 1:10 ratio to optimize the extraction of bioactive compounds. The maceration process was carried out for 24 h with occasional stirring, after which the filtrate was separated. This procedure was repeated using the same solvent for three consecutive days, and all filtrates obtained were combined. The combined filtrates were then evaporated using a rotary evaporator to remove the solvent until a viscous extract was obtained. Further concentration was carried out using a water bath until the extract reached an appropriate consistency for subsequent characterization [14].

Isolation of ulvan from *Ulva lactuca* linn

Green algae samples were obtained from a cultivation site in Sukabumi, West Java. The algae were sorted, thoroughly washed under running water, and air-dried indoors away from direct sunlight. The dried algae were ground and sieved through a 60-mesh sieve. A total of 200 g of algae powder was macerated in 400 mL of 96% ethanol for 24 h with occasional stirring to remove pigments and non-polar compounds. The resulting residue was then extracted with 2 L of distilled water, adjusted to pH 2 using HCl, and subsequently neutralized to pH 7 with NaOH. Extraction was carried out at 80 °C for 1 h at 90 rpm, followed by filtration to obtain the liquid extract. The extract was depigmented using 1% activated charcoal and filtered again. Further purification involved starch hydrolysis with 1 mL cellulase for 1 h and protein precipitation using ammonium sulfate. The solution was then concentrated using a rotary evaporator at 60 °C and dried in a vacuum oven at 70 °C to obtain the crude ulvan [15].

Biosynthesis of silver nanoparticles using *Moringa oleifera* leaf extracts and ulvan

The synthesis of silver nanoparticles (AgNPs) was carried out by adding ethanolic *Moringa oleifera* leaf extract at various concentrations such as 0.3% (E1), 0.4% (E2), 0.5% (E3), 0.6% (E4), and 0.7% (E5) as bio reducing agents into a 1.0 mM $AgNO_3$ solution. The concentrations of ethanolic *Moringa oleifera* leaf extract (0.3% - 0.7%) were selected based on a preliminary optimization approach [16,17]. The mixture was stirred using a magnetic stirrer at 300 rpm for 40 min while being heated on a hot plate at 50 - 60 °C. Subsequently, a 1% extract of green algae (*Ulva lactuca*) was added to the reaction mixture, followed by sonication for 30 min. The formation of AgNPs was indicated by the appearance of a dark brown color [18].

Characterization of silver nanoparticles

Maximum wavelength of silver nanoparticles

The Surface Plasmon Resonance (SPR) peak of the synthesized AgNP was determined using a UV-Vis spectrophotometer (Cecil CE 7410, UK). The AgNP suspensions from each formulation (E1 - E5) were appropriately diluted with distilled water to obtain absorbance values within the linear range of the instrument. Distilled water was used as the blank to record the baseline. Samples were placed in a 1 cm path length quartz cuvette, and the UV-Vis spectra were recorded in the wavelength range of 200 - 800 nm. The SPR peak was identified as the maximum absorbance (λmax) in the region of approximately 400 - 450 nm, corresponding to the characteristic SPR band of silver nanoparticles.

Zeta potential and particle size analysis of silver nanoparticles

Particle size and zeta potential of the synthesized nanoparticles were analyzed using Malvern ZSP (England) zeta sizer particle size.

Silver nanoparticle content

The AgNP suspension was first homogenized using a vortex mixer for approximately 1 minute. A 3 mL aliquot of the suspension was then mixed with 2 mL of concentrated HNO_3 and 0.5 mL of 30 %(w/v) H_2O_2, followed by microwave-assisted digestion using a four-step program: 5 min at 400 W, 8 min at 790 W, 4 min at 320 W, and 3 min without power. After digestion, the decomposed sample was diluted to a final volume of 25 mL with 0.2 %(v/v) HNO_3. The total silver content in the AgNP suspension was then analyzed using ICP-OES, and the silver concentration was expressed as mg/L. A blank solution was prepared following the same procedure but without the addition of the sample [19].

Antifungal activity test of silver nanoparticles using the well diffusion assay

The antifungal activity of silver nanoparticles (AgNPs) was evaluated using the well diffusion method

against *Candida albicans* ATCC 10231 obtained from the IPB Culture Collection (IPBCC). A total of 3.9 g of Potato Dextrose Agar (PDA) was dissolved in 100 mL of distilled water, sterilized, poured into Petri dishes, and allowed to solidify. The fungal culture was prepared by inoculating *C. albicans* ATCC 10231 onto sterile PDA and incubating at 30 °C for 24 h. The resulting culture was used as the test organism. After incubation, the fungal suspension was evenly spread over the surface of fresh sterile PDA plates using a sterile cotton swab to obtain a homogeneous lawn. Wells with a diameter of approximately 5 mm were then created in the agar, and 50 µL of the synthesized AgNP suspension was added into each well. The plates were incubated in an inverted position at 27 °C for 72 h (3×24 h^2). Antifungal activity was evaluated by measuring the diameter of the inhibition zones surrounding each well using a digital caliper.

Formulation of toothpaste containing AgNP-loaded alginate beads

The preparation of alginate beads was carried out based on research by [20] with slight modifications. 1 %(b/v) sodium alginate was dissolved in sterile distilled water using magnetic stirring until a homogeneous solution was obtained. The AgNP suspension was then added into the alginate solution according to the respective formula concentrations (0.3%, 0.4%, 0.5%, 0.6%, and 0.7% for F1 - F5), followed by gentle stirring to ensure uniform distribution of the nanoparticles. The AgNP-loaded alginate solution was subsequently dropped into a 2% calcium chloride solution to form beads through ionic gelation. The resulting beads were allowed to solidify for approximately 30 min, then filtered and rinsed with distilled water to remove excess calcium ions. The alginate beads were air-dried at room temperature for 24 h, followed by drying at 80 °C for 2 h [13].

The toothpaste was prepared using the dispersion method. Sodium carboxymethyl cellulose (Na-CMC) was slowly dispersed into warm distilled water until a homogeneous gel was formed. Sorbitol and glycerin were then added as humectants, and the mixture was homogenized thoroughly. Sodium benzoate and sodium saccharin were incorporated and stirred until completely dissolved. The abrasive agent, calcium carbonate, was gradually added while mixing to achieve a uniform, lump-free paste. Once the base paste was formed, sodium lauryl sulfate was added as a foaming agent and mixed gently to minimize foam formation. Flavoring agents and colorants were added as required to achieve the desired aroma and appearance. Finally, the AgNP-loaded alginate beads (1%) were incorporated into the toothpaste base and mixed slowly to maintain the structural integrity of the beads and ensure their uniform distribution throughout the formulation [21].

Characterization of AgNP-loaded alginate beads

FTIR analysis was performed to identify the functional groups present in the alginate beads containing silver nanoparticles (AgNPs) and to evaluate the interactions between the biomolecules and the nanoparticle matrix. Dried AgNP-loaded alginate beads were finely ground and mixed with (KBr). The mixture was then compressed into a transparent pellet. The pellets were analyzed using an FTIR spectrophotometer within the range of 4,000 - 400 cm^{-1} with a resolution of 4 cm^{-1}.

PXRD analysis was performed to determine the crystalline structure of the synthesized AgNPs. Measurements were carried out using an X-ray diffractometer. Data were collected over a 2θ range of 10° - 80° with a scanning rate of 2°/min.

Evaluation of toothpaste containing AgNP-loaded alginate beads

Organoleptic evaluation

Organoleptic evaluation of the toothpastes were assessed visually and sensorially, including color, odor, taste, and texture.

Homogeneity test

A small amount of toothpaste was placed between two glass slides and pressed gently. The sample was observed visually for the presence of coarse particles, phase separation, or uneven distribution of beads. The formulation was considered homogeneous if no visible lumps, agglomerates, or separated phases were observed.

pH and viscosity measurement

The pH of the toothpaste was measured using a calibrated digital pH-meter. Viscosity was determined

using a Brookfield viscometer equipped with an appropriate spindle at room temperature.

Spreadability test

Spreadability was evaluated using the glass plate weight method. Approximately 1 g of toothpaste was placed at the center of a glass plate, then covered with another glass plate. A 500 g load was placed on top and allowed to stand for 1 min. The diameter of the spread paste was measured in 2 perpendicular directions and averaged [4].

Foaming ability test

Foaming ability was assessed using the shake test method. 1 g of toothpaste was dispersed in 10 mL of distilled water in a graduated cylinder. The cylinder was closed and shaken vigorously for 1 min. The height of the produced foam was measured immediately after shaking. Foaming stability was assessed by measuring foam height again after 5 min [22].

The physical stability of the toothpaste formulations

The physical stability of the toothpaste formulations containing AgNP-loaded alginate beads was evaluated under room temperature storage conditions. Approximately 20 g of each formulation was filled into tightly closed laminated tubes and stored at room temperature, protected from direct light and excessive humidity. Observations were performed on day 0 **(**initial condition) and day 14 of storage. The formulations were visually inspected and evaluated for changes in in color, odor, homogeneity, pH, viscosity, spreadability and foaming ability.

Results and discussion

Extraction of moringa leaves and ulvan

The ethanolic extract of *Moringa oleifera* leaves obtained through maceration exhibited a deep green color, with a yield percentage of 23.7%. This yield value indicates a high concentration of bioactive compounds within the extract. In general, a higher extract yield reflects a higher level of active constituents successfully extracted. Moreover, the obtained yield meets the specifications of the Indonesian Herbal Pharmacopoeia (2017), which requires that the yield of thick extracts should not be less than 10% [23]. Similarly, the seaweed extraction process produced a green-colored extract with a yield of 19.3%, reflecting the effectiveness of the extraction process and adequate ulvan recovery.

Biosynthesis of silver nanoparticles using *Moringa oleifera* leaf extracts and ulvan

The synthesis of silver nanoparticles (AgNPs) in all formulations (E1 - E5) resulted in a color change of the reaction mixture from pale yellow to reddish-brown. This color transformation is a characteristic visual indicator of AgNP formation, which occurs through the reduction of silver ions (Ag^{+}) to metallic silver atoms (Ag^{0}) mediated by the bioactive molecules present in the plant extracts [24]. Secondary metabolites such as phenolic, flavonoids, saponins, and steroids act as the reducing agents in this process. The ethanolic extract of *Moringa oleifera* leaves functioned effectively as a bio reductant, as evidenced by the development of an intense color without the need for synthetic chemical reducing agents.

Characterization of silver nanoparticles

Maximum wavelength of silver nanoparticles

UV-Vis analysis revealed that all formulations (E1 - E5) exhibited the characteristic absorption bands of silver nanoparticles, with maximum wavelengths (λmax) falling within the visible region. According to [25], the quality of synthesized nanoparticles can be assessed by examining the intensity and position of the localized surface plasmon resonance (SPR) peak, which typically appears within the 380 - 450 nm range. Based on the results presented in the figure, an increase in λmax was observed with rising concentrations of *Moringa oleifera* extract used as the bioreducing agent. Formulation E1 displayed the lowest λmax, whereas E5 exhibited the highest value, and the difference between these formulations was statistically significant ($p < 0.05$).

The shift of λmax toward longer wavelengths (red-shift) in E3, E4, and particularly E5 indicates that the nanoparticles formed tend to be slightly larger in size or may have undergone changes in surface electron density. This red-shift phenomenon aligns with previous reports stating that an increase in particle size or aggregation level generally shifts the SPR peak to higher wavelengths [26]. The higher concentrations of *Moringa oleifera* leaf extract contribute to an increased

presence of reducing biomolecules such as polyphenols, flavonoids, phenolics, and alkaloids. While higher concentrations of these reducing agents accelerate Ag^0 nucleation, they may also facilitate further growth of the particle nuclei, resulting in slightly larger nanoparticles [27,28], as reflected by the elevated λmax values in E4 and E5. Despite the variations in λmax across formulations, the relatively narrow absorption bands observed in all samples indicate that the resulting nanoparticles possess a fairly uniform size distribution. This suggests that ulvan biomolecules function effectively as stabilizing (capping) agents, maintaining the colloidal stability of the synthesized nanoparticles.

Table 1 Characterization of silver nanoparticles synthesized using *Moringa oleifera* leaf extract and ulvan.

Extract's concentration	Maximum wavelength (nm)	Particle size (nm)	Zeta potential (mV)	Antifungal test (mm)	Silver content (mg/L)
E1	354.5 ± 0^{a}	699.03 ± 168.11^{a}	-5.1 ± 1.89^{a}	19.14 ± 0.70^{a}	-
E2	421.33 ± 2.88^{b}	441.86 ± 7.21^{a}	-4.9 ± 0.55^{a}	20.59 ± 0.30^{bc}	-
E3	420.16 ± 1.15^{b}	438.76 ± 6.67^{a}	-7.7 ± 6.35^{a}	21.28 ± 0.13^{bc}	6.01 ± 0.08
E4	416.66 ± 1.75^{b}	564.86 ± 134.63^{a}	-6.6 ± 3.06^{a}	19.88 ± 0.20^{ab}	-
E5	428.33 ± 2.36^{c}	587.63 ± 70.69^{a}	-12.6 ± 1.11^{a}	21.98 ± 0.07^{c}	-

Zeta potential and particle size analysis of silver nanoparticles

Particle size analysis revealed that the synthesized particles from all formulations (E1 - E5) exhibited average diameters ranging from 438.76 ± 6.67 nm to 699.03 ± 168.11 nm, with E1 producing the largest particles and E2 - E3 yielding relatively smaller ones. Nevertheless, statistical evaluation showed no significant differences among all formulations, indicating that used variations in *Moringa oleifera* extract concentration did not produce a meaningful effect on particle diameter. According to [29], nanoparticles are defined as particles measuring between 1 - 100 nm, and the much larger values observed in this study suggest the occurrence of particle aggregation. This interpretation is further supported by the broad SPR peaks obtained from UV-Vis spectroscopy, which typically reflect polydispersity and aggregated nanoparticle populations. Aggregation commonly occurs in green synthesis systems, where nanoparticle stabilization relies on natural biomolecules whose composition and concentration may vary. The zeta potential measurements further support the aggregation phenomenon. The zeta potential values of the five formulations ranged from –4.9 ± 0.55 mV to –12.6 ± 1.11 mV, with E5 showing the most negative surface charge. In general, colloidal systems with zeta potential values above ±30 mV is considered highly stable due to strong electrostatic repulsion [30]. Conversely, values close to zero reflect weaker repulsive forces and a greater tendency for aggregation [31]. The zeta potential values recorded in this study fall within the low electrostatic stability range, which is consistent with the observation of larger particle sizes and potential agglomeration. Despite E5 exhibiting a more negative zeta potential than the other formulations, its value still does not reach the threshold required to ensure robust colloidal stability, explaining why aggregation remained evident across all samples.

Silver nanoparticle content

Silver content analysis was performed on sample E3, which was selected because it exhibited the smallest particle size among the five formulations, and therefore was considered to represent the most efficient synthesis conditions. ICP-OES analysis showed that the silver concentration in E3 was 6.01 ± 0.08 mg/L. This value indicates that a portion of the Ag^+ ions was successfully reduced and incorporated into the nanoparticles. In relation to the smaller particle size observed in E3, this silver content suggests that the reduction process in this formulation was more effective than in the others. However, further optimization is still required to enhance reduction efficiency and achieve better control over particle size.

Antifungal activity test of silver nanoparticles using the well diffusion assay

The antifungal activity assay demonstrated that all AgNP formulations (E1 - E5) produced inhibition zones ranging between 19 - 22 mm. These inhibition zone diameters are consistent with findings reported by [5], who observed that various concentrations of AgNPs using *Aloe vera* extract generated inhibition zones between 10 and 22 mm against *Candida albicans* ATCC 10231. E2 and E3 exhibited significantly higher antifungal activity compared with E1, indicating AgNPs in suspension have the potential to adhere to and penetrate fungal hyphae, ultimately causing structural damage and cell death. This inhibitory mechanism is largely attributed to silver ions (Ag^+), which disrupt membrane-associated enzymes, including those involved in the respiratory chain. Additionally, Ag^+ can alter the expression of microbial proteins and enzymes and is known to interfere with DNA replication. AgNPs may also interact with substrates through competitive inhibition mechanisms, leading to enzyme inactivation and preventing the production of essential metabolites required for fungal survival [32]. Although variations in particle size were observed among the different formulations, these results indicate that the biological activity of the AgNPs is influenced more strongly by the composition of reducing and stabilizing biomolecules than by particle size alone.

In comparison, AgNPs synthesized via chemical reduction have been reported to exhibit antimicrobial activity against multidrug-resistant *Acinetobacter baumannii* with inhibition zone diameters ranging from 13 to 18 mm [33]. Although this comparison involves different microbial targets, the inhibition zones obtained in the present study (19 - 22 mm) are of similar or greater magnitude. This observation suggests that green-synthesized AgNPs prepared using *Moringa oleifera* extract and ulvan can achieve antimicrobial effectiveness comparable to chemically synthesized AgNPs, while offering the additional advantage of an environmentally friendly synthesis approach.

Characterization of AgNP-loaded alginate beads

The FTIR spectrum of alginate beads containing silver nanoparticles (AgNPs) at various concentrations (0.3% - 0.7%) as seen in **Figure 1** showed similar absorption patterns across all samples, indicating that the main chemical structure of the alginate matrix remained stable during the bead formation process and the addition of AgNPs. All spectra show a broad absorption band in the range of 3,546 - 3,404 cm^{-1}, which originates from O–H stretching vibrations. The width of this band reflects the presence of extensive hydrogen bonds in the alginate network and indicates that the addition of AgNPs does not interfere with the presence of hydroxyl groups in the polymer. The difference between AgNP concentrations is mainly seen in the change in band intensity at 1,617 cm^{-1}, which indicates asymmetric COO^- stretching vibrations, and 1,401 cm^{-1}, which indicates symmetric COO^- stretching vibrations. Variations in these two bands indicate an interaction between the alginate carboxylate group and Ag^+ ions or the AgNP surface, which generally occurs through the formation of metal-carboxylate bonds. According to [2], this interaction is one of the strongest bonds between alginate and AgNPs, as indicated by the COO^- bands appearing at around 1,600 cm^{-1} (asymmetric) and 1,400 cm^{-1} (symmetric). In addition, the absorption band appearing at 1,124 cm^{-1}, which is characteristic of the C–O–C stretching of glycosidic bonds, was also consistent across all samples. The presence of this band indicates that the alginate backbone structure is preserved and does not undergo degradation.

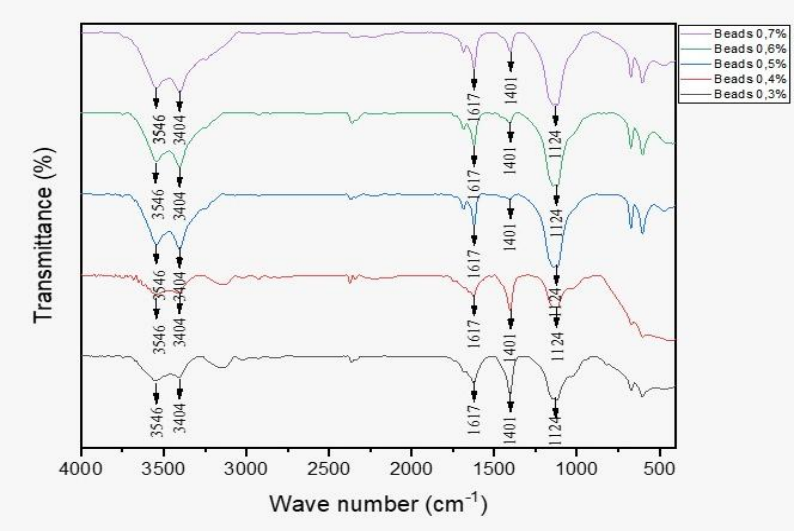

Figure 1 FTIR spectra of alginate beads incorporated wth silver nanoparticles (AgNPs) at various concentrations (0.3% - 0.7%).

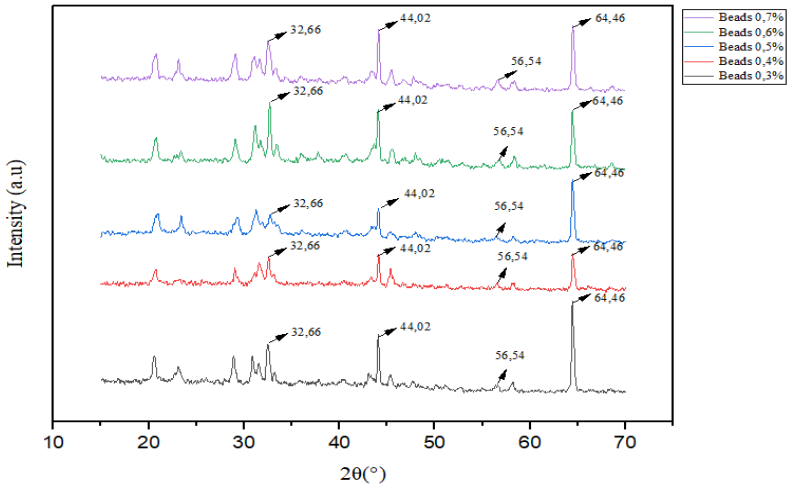

Figure 2 XRD patterns of alginate beads containing silver nanoparticles (AgNPs) at various concentrations (0.3% - 0.7%).

X-ray diffraction (XRD) testing of alginate beads containing silver nanoparticles (AgNPs) is shown in **Figure 4**. The results show a series of peaks with consistent positions across all samples, indicating that the crystalline structure of AgNPs is stably formed within the alginate matrix. All spectra show intense peaks at angles of approximately 32.66°, 44.02°, 56.54°, and 64.46°, which correspond to the (111), (200), (220), and (311) crystal planes of the typical face-centered cubic (FCC) structure of metallic silver [34]. The presence of a stable FCC crystal structure also indicates that the reduction of Ag^{+} is efficient and produces Ag^{0} in the form of nanoparticles distributed within the alginate matrix. In addition to the silver peaks, a series of additional peaks in the range of 20° - 32° originating from polysaccharide components such as alginate and ulvan are also visible [15]. These peaks reflect the semi-crystalline nature of the biopolymer, and their consistency indicates that the bead formation process and AgNP addition did not damage the polymer's basic structure. The relatively sharp diffraction peaks indicate the formation of nanoscale crystalline domains. Crystallite size was further estimated using the Scherrer equation (**Table 2**) with K = 0.9 and Cu Kα radiation (λ = 1.5406 A˚). Lattice strain was evaluated using the Williamson-Hall uniform deformation model (UDM), where the intercept corresponds to the crystallite size (D) and the slope represents the microstrain (ε). Based

on this analysis, the AgNPs exhibited crystallite sizes in the nanometer range and low lattice strain, indicating well-formed crystalline silver domains. Internal stress was further estimated. These results demonstrate that the AgNPs embedded within the alginate beads possess a stable FCC crystalline structure with nanoscale crystallite dimensions, supporting their suitability for antifungal toothpaste formulations.

Table 2 Crystallite size, microstrain, and internal stress of AgNP-loaded alginate beads determined by Scherrer and Williamson-Hall (W - H) analyses.

Sample beads	D Scherrer (nm)	D W - H (nm)	Microstrain (ε)	Stress (MPa)	R^2 W - H
E1	53.53	14.62	0.00360	298.70	0.590
E2	94.25	19.48	0.00243	201.50	0.351
E3	43.41	18.99	0.00219	181.60	0.353
E4	47.21	20.61	0.00199	165.18	0.484
E5	35.16	15.02	0.00285	236.14	0.412

Evaluation of toothpaste containing AgNP-loaded alginate beads

According to research conducted by [13], alginate beads containing AgNP can be used as antimicrobial biomaterials with low cytotoxicity and genotoxicity to human cells. Therefore, alginate beads containing AgNP are able to release AgNP slowly and in a controlled manner, thereby helping to reduce toxicity due to excessive silver ion release and functioning as an antimicrobial agent.

The organoleptic evaluation demonstrated that all toothpaste formulations containing AgNP-loaded alginate beads exhibited similar sensory characteristics. Visually, the formulations showed a uniform light green color, accompanied by a distinctive citrus aroma and taste, with no detectable metallic odor. The homogeneity test further confirmed that all formulations were uniform, both in the distribution of alginate beads and in the overall paste matrix, indicating successful dispersion and stability of the components.

Table 3 Physicochemical evaluation of toothpaste containing AgNP-loaded alginate beads.

Formula	Viscosity	pH	Spreadability (cm)	Foaming ability (cm)
F1	3693.33 ± 400.67^{a}	8.40 ± 0.10^{a}	6.37 ± 0.32^{b}	2.83 ± 0.29^{b}
F2	4106.67 ± 796.07^{ab}	8.60 ± 0.10^{ab}	6.30 ± 0.20^{b}	2.57 ± 0.15^{b}
F3	5413.33 ± 979.05^{abc}	8.90 ± 0.10^{c}	5.93 ± 0.23^{ab}	1.93 ± 0.21^{a}
F4	5806.67 ± 625.25^{bc}	8.87 ± 0.06^{bc}	5.90 ± 0.17^{ab}	2.37 ± 0.12^{ab}
F5	6646.67 ± 786.47^{c}	8.97 ± 0.15^{c}	5.70 ± 0.10^{a}	2.40 ± 0.35^{ab}

All values are presented as mean ± standard deviation (SD) from triplicate measurements (n = 3). Different superscript letters within the same column indicate statistically significant differences ($p < 0.05$).

The pH values of all formulations ranged from 8.40 ± 0.10 to 8.97 ± 0.15, remaining within the acceptable limits specified by the Indonesian National Standard (SNI 4.5 - 10.5). The slightly alkaline pH is typical of toothpastes containing calcium carbonate as an abrasive agent.

The viscosity values ranged from 3693.33 ± 400.67 cP to 6646.67 ± 786.47 cP. A gradual increase in viscosity was observed with higher concentrations of AgNPs encapsulated in the alginate beads, with F1 exhibiting the lowest and F5 the highest viscosity. This increase may be attributed to the greater number of beads incorporated into the matrix, leading to enhanced gel structural strength and increased physical interaction within the paste system, resulting in a denser consistency. Statistical analysis indicated significant differences between several formulations confirming

that higher AgNP concentrations contribute to increased viscosity.

The spreadability values ranged from 5.70 ± 0.10 cm to 6.37 ± 0.32 cm. Spreadability tended to decrease slightly as the concentration of AgNP-loaded beads increased, reflecting the inverse relationship between viscosity and spreadability. Nevertheless, all values remained within acceptable limits (5 - 7 cm), ensuring that the ease of application on the tooth surface was not compromised [35].

Foaming ability among the formulations ranged from 1.93 ± 0.21 cm to 2.83 ± 0.29 cm, considerably below the SNI maximum limit (<15 cm). These relatively low foam heights are still considered acceptable and adequate for cleansing, particularly due to the presence of sodium lauryl sulfate (SLS) as the foaming agent. Significant differences in foam height between F1 and F3 may be related to variations in viscosity and bead distribution. Formulations with higher viscosity tended to inhibit foam formation, resulting in slightly lower foam values.

Overall, these results indicate that the incorporation of AgNP-loaded alginate beads maintained satisfactory brushing performance and user-relevant sensory attributes. Therefore, the encapsulation approach did not negatively affect product usability, suggesting that the toothpaste formulations remain suitable for routine oral hygiene applications while delivering antifungal activity.

The physical stability of the toothpaste formulations

The stability study was conducted to ensure that the toothpaste containing AgNP-loaded alginate beads maintains its physical and chemical quality during storage. The presence of alginate beads and silver nanoparticles has the potential to influence the stability of the formulation. Therefore, this evaluation is essential to determine the consistency of product performance. The results of the stability assessment for the alginate bead–based toothpaste formulations are presented in **Table 4**.

Table 4 Physical stability of toothpaste formulations containing AgNP-loaded alginate beads over 14 days.

Parameter	Day nth	F1	F2	F3	F4	F5
Viscosity (cP)	0	3693.33 ± 549.30^{a}	3813.33 ± 931.52^{a}	4600.00 ± 700.57^{a}	5266.67 ± 775.20^{a}	5566.67 ± 883.25^{a}
	14	2806.67 ± 740.36^{a}	2860.00 ± 865.56^{a}	4246.67 ± 582.87^{a}	4460.00 ± 858.60^{a}	4880.00 ± 871.0^{a}
pH	0	8.47 ± 0.12^{a}	8.53 ± 0.15^{ab}	8.63 ± 0.15^{ab}	8.70 ± 0.10^{ab}	8.87 ± 0.15^{b}
	14	8.43 ± 0.12^{a}	8.43 ± 0.15^{a}	8.70 ± 0.20^{ab}	8.83 ± 0.15^{b}	8.90 ± 0.10^{b}
Spreadability (cm)	0	6.33 ± 0.15^{b}	6.20 ± 0.10^{ab}	6.00 ± 0.20^{ab}	5.90 ± 0.26^{ab}	5.77 ± 0.21^{a}
	14	6.43 ± 0.12^{a}	6.33 ± 0.15^{ab}	6.17 ± 0.15^{ab}	6.03 ± 0.21^{ab}	5.97 ± 0.15^{a}
Foaming ability (cm)	0	2.57 ± 0.15^{a}	3.00 ± 0.00^{ab}	3.33 ± 0.29^{b}	3.27 ± 0.25^{b}	3.37 ± 0.25^{b}
	14	1.80 ± 0.17^{a}	2.40 ± 0.35^{ab}	3.00 ± 0.00^{b}	2.57 ± 0.15^{b}	2.83 ± 0.29^{b}

All values are expressed as mean ± standard deviation (SD) from triplicate measurements (n = 3). Different superscript letters within the same row indicate statistically significant differences ($p < 0.05$).

Over the 14-day storage period, all formulations remained organoleptically stable, exhibiting no observable changes in color, odor, or homogeneity. Viscosity values showed a decrease across all formulations after 14 days of storage; however, all remained within the acceptable range specified by the Indonesian National Standard (SNI). This reduction in viscosity may be attributed to gel structure relaxation, interactions between humectants and polymeric components, or minor structural changes within the beads during storage.

The pH values of all formulations were relatively stable between day 0 and day 14, remaining within the SNI safety range, suggesting that the components within the toothpaste, including AgNPs and alginate beads, did not induce significant shifts in acidity or alkalinity.

Foam height also remained stable across all formulations, with only a slight reduction observed in some samples. This change was still within acceptable

limits and did not affect cleansing performance, as all values were far below the maximum SNI threshold (<15 cm). The consistency of foaming behavior during storage reflects the stability of the surfactant system within the formulations.

Based on the overall stability evaluation of the AgNP-based alginate bead toothpaste formulations, F3 demonstrated superior performance compared to the other four formulations. F3 met the criteria for a high-quality toothpaste in terms of organoleptic properties, homogeneity, viscosity, pH, spreadability, and foaming ability. Furthermore, although a slight decrease in viscosity was observed, the change remained within the acceptable range and was not substantially different from values measured on day 0 and day 14. Therefore, it can be concluded that the alginate beads containing AgNPs in the F3 formulation were able to maintain the physical stability of the toothpaste effectively.

Conclusions

This study demonstrated that silver nanoparticles (AgNPs) were successfully synthesized through a green synthesis method using *Moringa oleifera* leaf extract as a bioreductant and ulvan as a stabilizing agent, and could be effectively incorporated into alginate beads. Characterization using UV-Vis, FTIR, and PXRD confirmed the formation of AgNPs with a stable crystalline structure and the presence of metal-carboxylate interactions between the AgNPs and the alginate matrix. Toothpaste formulas containing alginate beads showed physical properties that met SNI standards, including pH, viscosity, spreadability, and foaming ability. All formulas were also organoleptically and physically stable during 14 days of storage at room temperature. Strong antifungal activity was found in all formulas, with formula E3 providing the best balance between physical stability, silver content, and antimicrobial effectiveness. Therefore, the results of this study demonstrate that green-synthesized alginate beads-based toothpaste formulas containing AgNPs have great potential as oral health products with effective antifungal activity and good physical stability.

Acknowledgements

This research was funded by the Regular Fundamental Research Grant of the Ministry of Education, Culture, Research, and Technology of the Republic of Indonesia, Fiscal Year 2024, under Grant No. 095/E5/PG.02.00.PL/2024.

Declaration of Generative AI in Scientific Writing

The authors acknowledge the use of generative AI tools (ChatGPT by OpenAI) in the preparation of this manuscript, specifically for language editing and grammar correction. No content generation or data interpretation was performed by AI. The authors take full responsibility for the content and conclusions of this work.

CRediT Author Statement

Nuur Aanisah: Methodology; Validation; Writing - Review & Editing; Visualization; Supervision. **Salsabila Jaya:** Software; Formal analysis; Investigation; Data Curation; Writing - Original Draft. **Evelyn Aprilly Tanan:** Formal analysis; Investigation; Data Curation; Writing - Original Draft. **Evi Sulastri:** Conceptualization; Validation; Resources; Supervision; Project administration.

References

[1] A Naganthran, G Verasoundarapandian, FE Khalid, MJ Masarudin, A Zulkharnain, NM Nawawi, M Karim, CAC Abdullah and SA Ahmad. Synthesis, characterization and biomedical application of silver nanoparticles. *Materials* 2022; **15(2)**, 427.

[2] S Lin, R Huang, Y Cheng, J Liu, BL Lau and MR Wiesner. Silver nanoparticle-alginate composite beads for point-of-use drinking water disinfection. *Water Research* 2013; **47(12)**, 3959-3965.

[3] OAK Ahmed, NRS Sibuyi, AO Fadaka, E Maboza, A Olivier, AM Madiehe, M Meyer and G Geerts. Prospects of using gum arabic silver nanoparticles in toothpaste to prevent dental caries. *Pharmaceutics* 2023; **15(3)**, 871.

[4] A Sevagaperumal, JR Joel and S Periyasamy. Formulation and evaluation of characteristics, remineralization potential, and antimicrobial properties of toothpaste containing nanohydroxyapatite and nanosilver particles: An *in vitro* study. *International Journal of Clinical Pediatric Dentistry* 2024; **17(6)**, 630-636.

[5] MMJ Arsène, PI Viktorovna, M Alla, M Mariya, SA Nikolaevitch, AKL Davares, ME Yurievna, M

Rehailia, AA Gabin, KA Alekseevna, YN Vyacheslavovna, ZA Vladimirovna, O Svetlana and D Milana. Antifungal activity of silver nanoparticles prepared using Aloe vera extract against Candida albicans. *Veterinary World* 2023; **16(1)**, 18-26.

[6] C Wang, YJ Kim, P Singh, R Mathiyalagan, Y Jin and DC Yang. Green synthesis of silver nanoparticles by *Bacillus methylotrophicus*, and their antimicrobial activity. *Artificial Cells, Nanomedicine, and Biotechnology* 2016; **44(4)**, 1127-1132.

[7] M Bindhu, M Umadevi, GA Esmail, NA Al-Dhabi and MV Arasu. Green synthesis and characterization of silver nanoparticles from *Moringa oleifera* flower and assessment of antimicrobial and sensing properties. *Journal of Photochemistry and Photobiology B: Biology* 2020; **205**, 111836.

[8] HM El-Rafie, MH El-Rafie and MK Zahran. Green synthesis of silver nanoparticles using polysaccharides extracted from marine macro algae. *Carbohydrate Polymers* 2013; **96(2)**, 403-410.

[9] H Perumalsamy, SR Balusamy, J Sukweenadhi, S Nag, D MubarakAli, M El-Agamy Farh, H Vijay and S Rahimi. A comprehensive review on *Moringa oleifera* nanoparticles: Importance of polyphenols in nanoparticle synthesis, nanoparticle efficacy and their applications. *Journal of Nanobiotechnology* 2024; **22**, 71.

[10] A Nicolae-Maranciuc, D Chicea and LM Chicea. Ag nanoparticles for biomedical applications—Synthesis and characterization—A review. *International Journal of Molecular Sciences* 2022; **23(10)**, 5778.

[11] M Asif, R Yasmin, R Asif, A Ambreen, M Mustafa and S Umbreen. Green synthesis of silver nanoparticles (AgNPs), structural characterization, and their antibacterial potential. *Dose-Response* 2022; **20(2)**, 15593258221088709.

[12] A Massironi, A Morelli, L Grassi, D Puppi, S Braccini, G Maisetta, S Esin, G Batoni, CD Pina and F Chiellini. Ulvan as novel reducing and stabilizing agent from renewable algal biomass: Application to green synthesis of silver nanoparticles. *Carbohydrate Polymers* 2019; **203**, 310-321.

[13] DP Mahasawat, S Mudtaleb and P Eaidprap. The influence of silver nanoparticle sizes on antibacterial activity, cytotoxicity and genotoxicity of alginate hydrogel beads containing silver nanoparticles. *Applied Mechanics and Materials* 2019; **886**, 70-77.

[14] FA Puspitasari, NB Kartikasari, S Mutiyastika, R Purnamasari, N Lusiana and E Agustina. Effect of different solvents in the extraction process of Kelor (*Moringa oleifera*) leaves on bioactive resources and phenolic acid content. *International Conference on Sustainable Health Promotion* 2023; **3(1)**, 167-178.

[15] E Sulastri, MS Zubair, R Lesmana, AFA Mohammed and N Wathoni. Development and characterization of ulvan polysaccharides-based hydrogel films for potential wound dressing applications. *Drug Design, Development and Therapy* 2021; **2021**, 4213-4226.

[16] Z Haris and I Ahmad. Green synthesis of silver nanoparticles using *Moringa oleifera* and its efficacy against gram-negative bacteria targeting quorum sensing and biofilms. *Journal of Umm Al-Qura University for Applied Sciences* 2024; **10**, 156-167.

[17] B Sadeghi and F Gholamhoseinpoor. A study on the stability and green synthesis of silver nanoparticles using *Ziziphora tenuior (Zt)* extract at room temperature. *Spectrochimica Acta Part A: Molecular and Biomolecular Spectroscopy* 2015; **134**, 310-315.

[18] E Sulastri, R Lesmana, MS Zubair, AFA Mohammed, KM Elamin and N Wathoni. Ulvan/Silver nanoparticle hydrogel films for burn wound dressing. *Heliyon* 2023; **9(7)**, 18044.

[19] RM Galazzi, EDB Santos, T Caurin, GDS Pessôa, IO Mazali and MAZ Arruda. The importance of evaluating the real metal concentration in nanoparticles post-synthesis for their applications: A case-study using silver nanoparticles. *Talanta* 2016; **146**, 795-800.

[20] N Kaur, B Singh and S Sharma. Hydrogels for potential food application: Effect of sodium alginate and calcium chloride on physical and

morphological properties. *The Pharma Innovation Journal* 2018; **7(7)**, 142-148.

[21] D Marlina and N Rosalini. Formulasi pasta gigi gel ekstrak daun sukun (*Artocarpus altilis*) dengannatrium cmc sebagai *Gelling agent* dan uji kestabilan fisiknya. *Portal Jurnal Poltekkes Palembang* 2017; **12(1)**, 36-50.

[22] J Ogboji, IY Chindo, A Jauro, DEA Boryo and NM Lawal. Formulation, physicochemical evaluation and antimicrobial activity of green toothpaste on streptococcus mutans. *International Journal of Advanced Chemistry* 2018; **6(1)**, 108-113.

[23] I Solihah, M Mardiyanto, S Fertilita, H Herlina and O Charmila. The standardization of ethanolic extract of Tahongai leaves (*Kleinhovia hospita* L.). *Science and Technology Indonesia* 2018; **3(1)**, 14-18.

[24] S Kwon and S Ko. Colorimetric freshness indicator based on cellulose nanocrystal–silver nanoparticle composite for Intelligent Food Packaging. *Polymers* 2022; **14(17)**, 3695.

[25] NS Alharbi, NS Alsubhi and AI Felimban. Green synthesis of silver nanoparticles using medicinal plants: Characterization and application. *Journal of Radiation Research and Applied Sciences* 2022; **15(3)**, 109-124.

[26] V Sharma, D Verma and GS Okram. Influence of surfactant, particle size and dispersion medium on surface plasmon resonance of silver nanoparticles. *Journal of Physics: Condensed Matter* 2020; **32(14)**, 145302.

[27] EO Dare, CO Oseghale, AH Labulo, ET Adesuji, EE Elemike, JC Onwuka and JT Bamgbose. Green synthesis and growth kinetics of nanosilver under bio-diversified plant extracts influence. *Journal of Nanostructure in Chemistry* 2015; **5**, 85-94.

[28] R Singh, A Gupta, V Patade, G Balakrishna, H Pandey and A Singh. Synthesis of silver nanoparticles using extract of *Ocimum kilimandscharicum* and its antimicrobial activity against plant pathogens. *SN Applied Sciences* 2019; **1**, 1652.

[29] PS Jassal, D Kaur, R Prasad and J Singh. Green synthesis of titanium dioxide nanoparticles: Development and applications. *Journal of Agriculture and Food Research* 2022; **10**, 100361.

[30] DJ Pochapski, C Carvalho dos Santos, GW Leite, SH Pulcinelli and CV Santilli. Zeta potential and colloidal stability predictions for inorganic nanoparticle dispersions: Effects of experimental conditions and electrokinetic models on the interpretation of results. *Langmuir* 2021; **37(45)**, 13379-13389.

[31] S Karmakar. Particle size distribution and zeta potential based on dynamic light scattering: Techniques to characterize stability and surface charge distribution of charged colloids. *Recent Trends in Materials: Physics and Chemistry* 2019; **28**, 117-159.

[32] AH Hashem, E Saied, BH Amin, FO Alotibi, AA Al-Askar, AA Arishi, FM Elkady and MA Elbahnasawy. Antifungal activity of biosynthesized silver nanoparticles (AgNPs) against *Aspergilli* causing aspergillosis: Ultrastructure study. *Journal of Functional Biomaterials* 2022; **13(4)**, 242.

[33] PC Pandey, AK Tiwari, MK Gupta, G Pandey and RJ Narayan. Effect of the organic functionality on the synthesis and antimicrobial activity of silver nanoparticles. *Nano LIFE* 2020; **10(3)**, 2050002.

[34] MA Alam, SI Sadia, MKH Shishir, RK Bishwas, S Ahmed, SM Al-Reza and SA Jahan. Crystallinity integration and crystal growth behavior study of preferred oriented (111) cubic silver nanocrystal. *Inorganic Chemistry Communications* 2025; **173**, 113834.

[35] B Gratia, P Veronika, Y Yamlean, K Lifie and R Mansauda. Formulation of toothpaste of nutmeg ethanol extract (*Myristica fragrans* Houtt.). *Pharmacon* 2021; **10(3)**, 968-974.